View metadata, citation and similar papers at core.ac.uk
brought to you by CORE
provided by University of Queensland eSpace

ChemPubSoc Europe
DOI: 10.1002/cssc.201601603
Communications

Switched Photocurrent on Tin Sulfide-Based Nanoplate Photoelectrodes

Hongjun Chen,[a] Miaoqiang Lyu,[a] Meng Zhang,[a] Krishna Feron,[b, c] Debra J. Searles,[d] Matthew Dargusch,[e] Xiangdong Yao,[f] and Lianzhou Wang*[a]

A new type of SnS_2 nanoplate photoelectrode is prepared by using a mild wet-chemical method. Depending on the calcination temperatures, SnS_2-based photoelectrodes can either retain their n-type nature with greatly enhanced anodic photocurrent density (ca. 1.2 mA cm^{-2} at 0.8 V vs. Ag/AgCl) or be completely converted into p-type SnS to generate approximately 0.26 mA cm^{-2} cathodic photocurrent density at −0.8 V vs. Ag/AgCl. The dominance of sulfur and tin vacancies are found to account for the dramatically different photoelectrochemical behaviors of n-type SnS_2 and p-type SnS photoelectrodes. In addition, the band structures of n-type SnS_2 and p-type SnS photoelectrodes are also deduced, which may provide an effective strategy for developing SnS_2/SnS films with controllable energy-band levels through a simple calcination treatment.

In light of the fast development of a global economy and an increasing global population, energy shortage and deterioration of the environment are emerging among the most important challenges for humans. Concerns over climate change and the exhausting supply of fossil fuels have triggered ever-increasing interest towards sustainable energy supply in recent years.[1,2] Among the possible solutions for sustainable energy generation, solar energy stands out as one of the most promising options due to its abundance and availability.[3–6] To fully utilize solar energy for the generation of H_2, various semiconductors have been reported as photoelectrodes for photoelectrochemical water splitting.[7,8] Among them, the most well-studied photoelectrodes have been n-type semiconductors, whereas many p-type semiconductors are quite expensive, involve relatively difficult processes, and are less stable.[6,9–11] Therefore, identification and further development of cost-effective p-type semiconductors with a simple fabrication process and suitable band gap and conduction band position have attracted tremendous interest.[12,13]

To develop smart electronic devices, different stimuli have been adopted to trigger a signal change and further used to design various switchable systems.[14] To date, several stimuli including potential, wavelength, and pH value are applied to switch the photocurrent direction.[15–17] Recently, new systems, such as hybrid n-/p-type semiconductors,[18] TiO_2-supported Au nanoparticles,[19] and TiO_2-supported Ag nanoclusters,[20] have been reported to tune the photocurrent direction. However, transforming n-type semiconductors into p-type semiconductors by controlling the calcination temperature and further switching the photocurrent has rarely been reported.

Herein we report the cost-effective fabrication of a new p-type SnS nanoplate photoelectrode directly on a fluorine-doped tin oxide (FTO) substrate through a simple wet-chemical method. Unlike traditional techniques such as plasma-enhanced chemical vapor deposition,[21] chemical bath deposition,[22] cathodic electrodeposition,[23] and spray pyrolysis,[24] the fabrication of the SnS photoelectrode in this study was realized by the transformation of n-type SnS_2 into p-type SnS under inert Ar gas at a relatively elevated temperature, which not only provides a simple method for the fabrication of the SnS photoelectrode at a low cost, but also grows SnS directly on a rigid substrate with effective control of the morphology. there are two steps for the fabrication of p-type SnS nanoplate photoelectrodes (Scheme 1). The first step is a wet-chemical method for the direct growth of a SnS_2 nanoplate on an FTO substrate. The second step is a simple post-calcination treatment of the SnS_2 on FTO (SnS_2/FTO). The proposed two-step method can effectively avoid the inherent problem of the oxidation of Sn^{2+} to Sn^{4+} under high-temperature synthetic processes in a one-step method by using Sn^{4+} rather than Sn^{2+} as the precursor. Interestingly, the photocurrent density of the SnS_2/FTO photoelectrode after low-temperature calcination (300 °C) can be significantly increased to 1.2 mA cm^{-2} at 0.8 V vs. Ag/AgCl, which is much higher than that of the as-synthe-

[a] Dr. H. Chen, M. Lyu, M. Zhang, Prof. L. Wang
Nanomaterials Centre, School of Chemical Engineering and Australian Institute for Bioengineering and Nanotechnology
The University of Queensland, Brisbane, QLD 4072 (Australia)
E-mail: l.wang@uq.edu.au
[b] Dr. K. Feron
CSIRO Energy
Newcastle, NSW 2300 (Australia)
[c] Dr. K. Feron
Centre for Organic Electronics, The University of Newcastle
Callaghan, NSW, 2308 (Australia)
[d] Prof. D. J. Searles
Centre for Theoretical and Computational Molecular Science, School of Chemistry and Molecular Biosciences and Australian Institute for Bioengineering and Nanotechnology, The University of Queensland
Brisbane, QLD 4072 (Australia)
[e] Prof. M. Dargusch
Centre for Advanced Materials Processing and Manufacture, School of Mechanical and Mining Engineering, The University of Queensland
Brisbane, QLD 4072 (Australia)
[f] Prof. X. Yao
School of Natural Sciences and Queensland Micro- and Nanotechnology Centre (QMNC), Griffith University, Nathan Campus
Brisbane, QLD 4111 (Australia)
Supporting information for this article can be found under: http://dx.doi.org/10.1002/cssc.201601603.

© 2017 Wiley-VCH Verlag GmbH & Co. KGaA, Weinheim

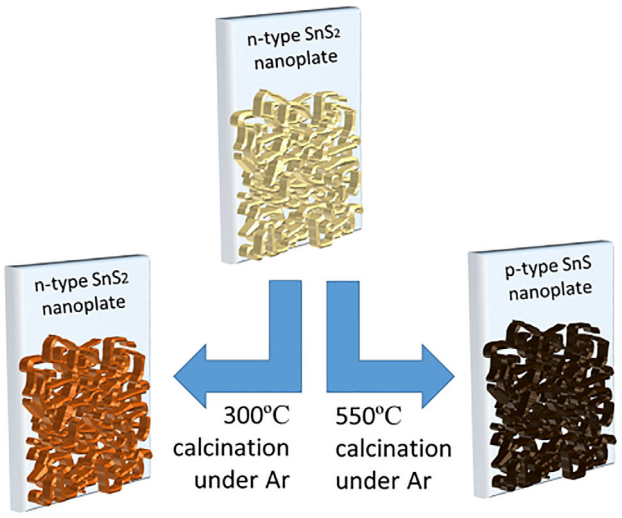

Scheme 1. Fabrication process for the SnS_2 nanoplate/FTO and SnS nanoplate/FTO photoelectrodes.

sized SnS_2/FTO photoelectrode. Alternatively, with high-temperature calcination (550 °C) the SnS_2/FTO photoelectrode can be transformed into a p-type SnS nanoplate photoelectrode (SnS/FTO) and generate a cathodic photocurrent, which is totally different from the anodic photocurrent generated on the as-synthesized, low-temperature calcined SnS_2/FTO photoelectrodes. To our knowledge, investigations of the transformation of n-type SnS_2 nanoplates into p-type SnS nanoplates and their related photoelectrochemical performances have very seldom been reported.

After 2 h of calcination at 300 °C or 550 °C in Ar, the color of the as-prepared SnS_2/FTO glass changed from yellow into brownish or totally black, respectively (Figure 1, inset). Correspondingly, the optical absorption of these three samples (Figure 1 a) reveals that the absorption onset of the as-prepared SnS_2/FTO is associated with a band gap of around 2.6 eV, which was decreased by roughly 0.4 eV after the calcination at 300 °C and further decreased by around 0.8 eV after the calcination at 550 °C. The band gaps of both calcined samples are in good agreement with the typical reported values for SnS_2 (2.24 eV) and SnS (1.11 eV),[25] respectively. The X-ray diffraction (XRD) was used to identify the crystallinity and phase structure of the as-synthesized and calcined samples. Here, normal glass substrates were used for the growth of the SnS_2 thin films in order to avoid the interference of FTO signals produced from the substrate. The XRD peaks of the as-prepared sample (Figure 1 b) can be indexed to hexagonal SnS_2 (JCPDS No. 21-1231). After calcination at 300 °C for 2 h, the phase of SnS_2 was retained, but the crystallinity was greatly improved as demonstrated with much narrower XRD peaks with higher intensity. Unlike those of SnS_2, the XRD peaks of the sample calcined at 550 °C for 2 h can be indexed into herzenbergite SnS (JCPDS No. 33-1375), suggesting the SnS_2 phase is completely converted into SnS. From the XRD analysis, it is clear that the band gap change for SnS_2 before and after calcination at 300 °C could be attributed to an increase in the film density and sulfur deficiency or tin vacancy.[25] A similar band gap change was also reported by Hanini et al. for the annealed anatase TiO_2.[26] In terms of the band gap change before and after calcination at 550 °C, the samples should be treated as two different semiconductors with different band gaps.

The morphologies of the SnS_2/FTO photoelectrodes before and after calcination were characterized by scanning electron microscopy (SEM). SnS_2 nanoplates were interconnected to each other and distributed uniformly on the whole FTO substrate surface (Figure 2 a). The nanoplates are quite thin and their thickness is normally less than 20 nm (inset in Figure 2 a). After calcination at 300 °C or 550 °C, the morphology of the SnS_2/FTO or SnS/FTO that is obtained remained nearly intact (Figure 2 b and c), with only the edge of the nanoplate becoming slightly rougher (inset in Figure 2 b), or even splitting into small bunches (inset in Figure 2 c). From the cross-sectional

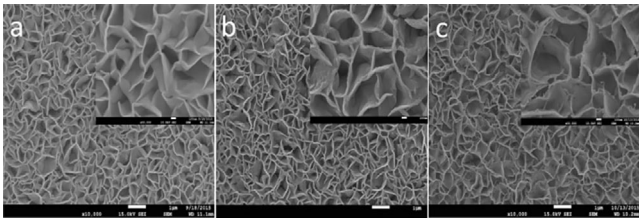

Figure 2. SEM images of SnS_2 nanoplates without calcination (a) and after calcination at 300 °C (b) and at 550 °C (c). The scale bar is 1 μm. The insets are the magnified SEM images for which the scale bar is 100 nm.

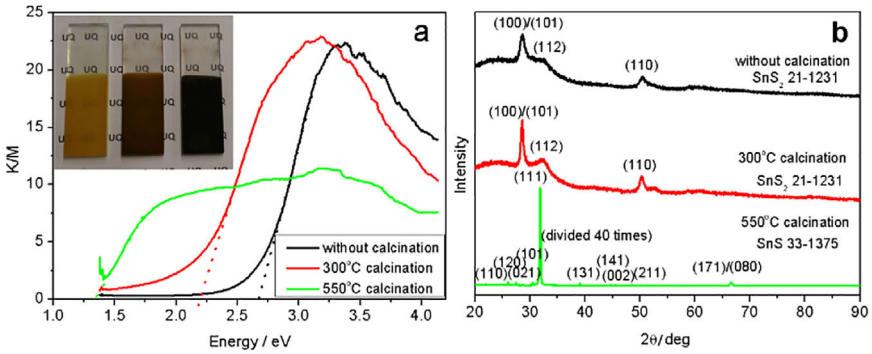

Figure 1. UV/Vis spectra (a) and XRD patterns (b) of SnS_2 without calcination and after calcination at 300 °C and at 550 °C. The inset in (a) is the photograph of SnS_2/FTO without calcination (left) and after calcination at 300 °C (middle) and at 550 °C (right).

© 2017 Wiley-VCH Verlag GmbH & Co. KGaA, Weinheim

images (see the Supporting Information, Figure S1), the two-dimensional nanoplates that were densely and vertically grown on the FTO surface were around 1.5 μm in height. The height of the two-dimensional nanoplate has little obvious change after calcination. Energy dispersive spectroscopy (EDS) was also conducted to analyze the components in the samples. The three samples mainly contained Sn, S and some O (see the Supporting Information, Figure S2), which might have originated from the underlying FTO substrate. Owing to the microporous structure of the film and the interference of the FTO substrate, the atomic ratio between Sn and S did not strictly follow the molecular formula. However, the change of the atomic ratio between Sn and S was obvious and the atomic ratio of Sn to S increased on increasing the calcination temperature from room temperature to 300 °C and then to 550 °C.

Figure 3 shows the current density–potential (*J–V*) curves for the three different photoelectrodes in 1 M Na_2SO_4 solution under chopped sunlight (AM 1.5, 100 mW cm^{-2}). When a potential scan was applied from −0.4 V to 0.8 V vs. Ag/AgCl, an anodic photocurrent was generated on the SnS_2/FTO photoelectrodes prepared without calcination and those prepared with calcination at 300 °C (Figure 3 a). The photocurrent density of the SnS_2/FTO photoelectrode was greatly enhanced after calcination and the photocurrent density reached about 1.2 mA cm^{-2} at 0.8 V vs. Ag/AgCl, suggesting that the calcination treatment reduced the defect density and increased the interparticle contacts and/or improved the contact between the interface of SnS_2 and the FTO substrate, which further facilitates the excited charge transfer.[27] In contrast, after the SnS_2/FTO photoelectrode was calcined at 550 °C, the resultant SnS/FTO photoelectrode had almost no photoresponse under the same experimental conditions. When the potential was scanned from 0 to −0.8 V vs. Ag/AgCl in 1 M Na_2SO_4, the anodic photocurrent gradually decreased to zero within the potential range between 0 and −0.4 V on the SnS_2/FTO photoelectrodes prepared without calcination and with calcination at 300 °C. For the SnS/FTO photoelectrode, a cathodic photocurrent appeared and gradually increased within the potential range from −0.4 to −0.8 V vs. Ag/AgCl and the photocurrent density reached ca. 0.26 mA cm^{-2} at −0.8 V vs. Ag/AgCl. The observed photoelectrochemical behavior of the SnS_2/FTO and SnS/FTO photoelectrodes suggested that SnS_2/FTO photoelectrode was a typical n-type semiconductor whereas SnS/FTO photoelectrode was a p-type semiconductor. To verify this, the Mott–Schottky (MS) curves were measured and the capacitance was derived from the electrochemical impedance obtained at each potential and a frequency of 5 kHz in the dark. The SnS_2/FTO photoelectrode formed after calcination at 300 °C gave rise to a positive slope (see the Supporting Information, Figure S3), indicating n-type nature, which is the same as that of the SnS_2/FTO photoelectrode formed without calcination. In contrast, the photoelectrode formed after calcination at 550 °C gave a negative slope, suggesting a p-type nature of the SnS/FTO photoelectrode. The results of the MS measurements were in agreement with the photoelectrochemical behavior of these photoelectrodes (Figure 3). From the above characterizations, it is very clear that the n-type SnS_2/FTO photoelectrode remained n-type after calcination at 300 °C, but was transformed into p-type SnS/FTO after calcination at 550 °C.

To explore the electrochemical behavior under chopped light, the amperometric current density–time (*J–T*) and the open-circuit potential (OCP) of both the calcined SnS_2/FTO and SnS/FTO photoelectrodes were measured. The SnS_2/FTO photoelectrode exhibited an anodic photocurrent during three cycles of intermittent chopped irradiation, whereas the SnS/FTO photoelectrode had almost no response under the same conditions with an applied potential of 0.6 V vs. Ag/AgCl (Figure 4 a). In contrast, when a negative bias (−0.5 V vs. Ag/AgCl) was applied, the SnS/FTO photoelectrode showed a significant cathodic photocurrent under chopped light, but the SnS_2/FTO photoelectrode exhibited a very weak anodic photocurrent (Figure 4 b). Therefore, it is further confirmed that the SnS_2/FTO and SnS/FTO photoelectrodes demonstrate typical photoresponses of n- and p-type photoelecrodes, respectively. The OCP values of both photoelectrodes were also measured (Figure 4 c). When illuminated under light, the OCP value of the SnS_2/FTO photoelectrode quickly shifted to a more negative value, suggesting increasing negative charge within the photoelectrode. In contrast, the OCP value of the SnS/FTO photoelectrode shows a slightly positive shift, indicating some positive charge was formed during the light irradiation. These behaviors are consistent with those of typical n- and p-type photoelectrodes, respectively, which provides further evidence that the SnS_2/FTO is a typical n-type photoelectrode and the SnS/FTO is a typical p-type photoelectrode. The above characteriza-

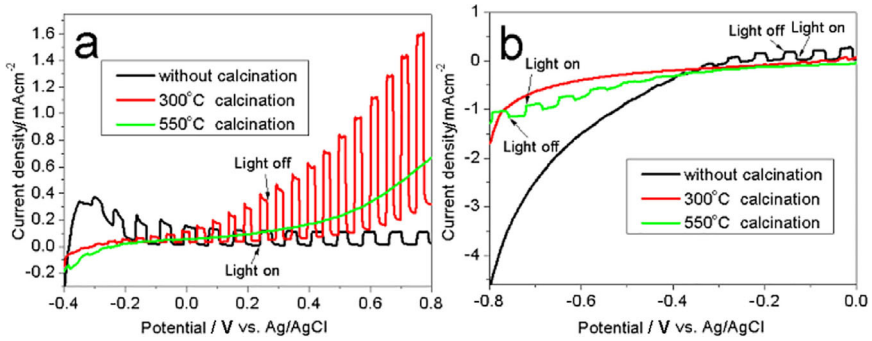

Figure 3. *J–V* curves of SnS_2/FTO without calcination (black) and after calcination at 300 °C (red) and at 550 °C (green).

© 2017 Wiley-VCH Verlag GmbH & Co. KGaA, Weinheim

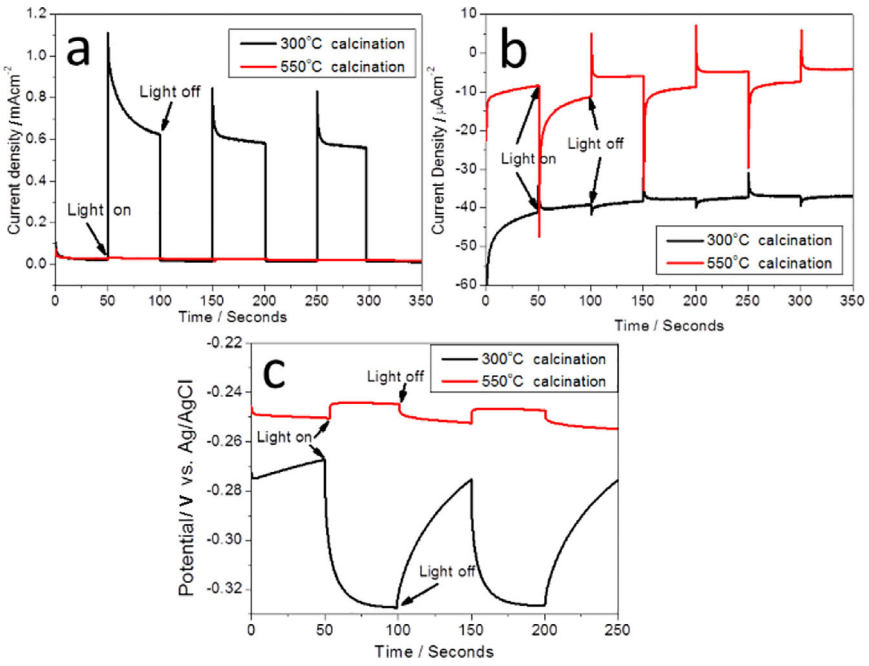

Figure 4. *J–T* curves (a and b) and OCP (c) of SnS_2/FTO after calcination at 300 °C (black) and at 550 °C (red), respectively. Applied potentials were 0.6 and −0.5 V vs. Ag/AgCl for (a) and (b), respectively.

tion establishes that a wet-chemical-synthesized SnS_2/FTO photoelectrode can retain its n-type character if calcination occurs at low temperatures (300 °C), but can be converted into a p-type SnS/FTO under high calcination temperatures (550 °C). This indicates that when the temperature was increased from 300 °C to 550 °C, SnS_2 dissociation began to occur and S depletion and high temperatures promoted the dissociation processes until SnS finally formed.[28] The formation of SnS could proceed as follows:

$$SnS_2 \xrightarrow{\Delta} SnS + \frac{1}{x}S_x$$

where $x = 2–8$ and represents the various S species that can be formed during this process. For the transformation from n-type SnS_2 into p-type SnS, it is generally accepted that a reducible cation such as Sn^{4+} is associated with electron conduction of the n-type semiconductor, whereas an oxidizable cation such as Sn^{2+} is connected with hole conduction of the p-type semiconductor.[25,29,30] The dominance of sulfur and tin vacancies in SnS_2 and SnS, respectively, relate to the differing behaviors observed since the sulfur vacancies act as electron traps and Sn vacancies act as acceptor defects.[25] Therefore, SnS_2 and SnS are typical n- and p-type semiconductors, respectively.

To determine the valence band position for the three photoelectrodes, photoelectron spectroscopy in air (PESA) measurements were conducted. The valence bands were detected at −5.86, −5.65, and −5.40 eV vs. the vacuum level for the SnS_2/FTO photoelectrode before calcination and after calcination at 300 °C or 550 °C (or SnS/FTO), respectively (see the Supporting Information, Figure S4). Therefore, the valence and conduction band positions for these three different SnS_2 and SnS semiconductors can be clearly determined based on their optical band gaps derived from UV/Vis spectroscopy (Figure 1 a) and valence band positions from PESA (Figure S4). From the band diagram for these three semiconductors (see the Supporting Information, Figure S5), it can be concluded that the annealing treatment significantly affects the energy band levels of the films. Elevating the annealing temperature raises the valence band positions. This observation may provide an effective strategy for developing SnS_2/SnS films with controllable energy band levels through a simple calcination step.

In summary, we have reported a facile wet-chemical method for the direct synthesis of SnS_2 nanoplates on an FTO substrate. More importantly, we found that a simple post-annealing treatment process carried out on the SnS_2 nanoplates had a significant effect on both the chemical composition and the intrinsic semiconducting properties of the nanoplates produced. When we used low-temperature calcination (300 °C), SnS_2 retained its n-type nature and a remarkably enhanced anodic photocurrent density (1.2 mA cm^{-2} at 0.8 V vs. Ag/AgCl) was achieved compared to that of the non-annealed sample. In contrast, the n-type SnS_2 nanoplates were transformed into p-type SnS nanoplates with the generation of cathodic photocurrent after high-temperature calcination (550 °C). The new findings reported herein may provide insights for designing new generation devices with potential applications in solar cells, photodetectors, and other optoelectronic areas.

Experimental Section

The fabrication procedure

The fabrication of the n-type SnS_2 nanoplates and p-type nanoplates of SnS photoelectrodes was performed as follows. One clean FTO glass plate with the conductive side facing down was im-

© 2017 Wiley-VCH Verlag GmbH & Co. KGaA, Weinheim

mersed in an ethanol solution containing 0.05 M $SnCl_4 \cdot 4H_2O$ and 0.1 M thioacetamide in a closed container at 80 °C for 2 h. After thoroughly rinsing the surface, the as-prepared SnS_2/FTO photoelectrode was transferred into a tube furnace under Ar gas and the temperature was gradually raised from room temperature to 300 °C or 550 °C at a ramping rate of 1 °C min^{-1}. The samples were then kept for 2 h at the highest temperature to ensure the transformation was completely finished, then allowed to cool naturally to room temperature. Given the ultrathin nature of the nanoplates, heat treatment of 2 h should be sufficient for the phase transformation to finish, as evidenced by the XRD patterns. After thoroughly rinsing their surfaces with Millipore water, the SnS_2/FTO or SnS/FTO photoelectrodes were directly used for photoelectrochemical measurements.

Characterization

UV/Vis absorption spectra were recorded with a V650 spectrophotometer (JASCO). X-ray diffraction (XRD) patterns were collected on a diffractometer (Miniflex, Rigaku). Scanning electron microscopy (SEM) and energy dispersive spectroscopy (EDS) measurement were performed on JEOL JSM-7001F. The ionization potential of the semiconductors was determined by using a Riken Keiki AC2 photoelectron spectroscopy in air (PESA) system.[31] Thin films were deposited on FTO glass and the photoelectron yield was measured as a function of energy. The ionization potential was determined from these results by fitting two linear lines and finding their intersection (Figure S4).[32]

Photoelectrochemical measurements

Photoelectrochemical measurements were performed in a homemade one-compartment reactor with a quartz window. A three-electrode configuration was used with Pt wire, Ag/AgCl, and SnS_2/FTO or SnS/FTO as the counter, reference, and working electrodes, respectively. N_2-saturated 1 M aqueous Na_2SO_4 solution (pH 6) was used as the electrolyte. Amperometric *J–T* curves were measured at 0.6 or −0.5 V vs. Ag/AgCl on an Electrochemical Workstation (CHI660d). A xenon lamp (150 W, Newport) with an AM 1.5G filter was used as the light source for the measuring the photocurrent. The illumination area was set by an aperture to 0.785 cm^2. The Mott–Schottky analysis was performed in a three-electrode configuration in 1 M Na_2SO4 solution with 5 kHz frequency in the dark.

Acknowledgements

The Australian Research Council is acknowledged for its financial support through its Discovery, Linkage, and Future Fellowship projects, and Dr. H. J. Chen thanks the University of Queensland for the UQ Postdoctoral Fellowship grant support.

Keywords: calcination · nanostructures · photoelectrochemistry · semiconductors · tin

[1] L. Freris, D. Infield, *Renewable Energy in Power Systems*, Wiley, Chichester, **2009**, p. 2.
[2] P. V. Kamat, *J. Phys. Chem. C* **2007**, *111*, 2834 – 2860.
[3] M. Grätzel, *Nature* **2001**, *414*, 338 – 344.
[4] B. E. Hardin, H. J. Snaith, M. D. McGehee, *Nat. Photonics* **2012**, *6*, 162 – 169.
[5] T. R. Cook, D. K. Dogutan, S. Y. Reece, Y. Surendranath, T. S. Teets, D. G. Nocera, *Chem. Rev.* **2010**, *110*, 6474 – 6502.
[6] M. G. Walter, E. L. Warren, J. R. McKone, S. W. Boettcher, Q. Mi, E. A. Santori, N. S. Lewis, *Chem. Rev.* **2010**, *110*, 6446 – 6473.
[7] A. Kudo, Y, Miseki, *Chem. Soc. Rev.* **2009**, *38*, 253 – 278.
[8] R. Marschall, L. Wang, *Catal. Today* **2014**, *225*, 111 – 135.
[9] O. Khaselev, J. A. Turner, *J. Electrochem. Soc.* **1998**, *145*, 3335 – 3339.
[10] M. H. Lee, K. Takei, J. Zhang, R. Kapadia, M. Zheng, Y.-Z. Chen, J. Nah, T. S. Matthews, Y.-L. Chueh, J. W. Ager, A. Javey, *Angew. Chem. Int. Ed.* **2012**, *51*, 10760 – 10764; *Angew. Chem.* **2012**, *124*, 10918 – 10922.
[11] B. Seger, T. Pedersen, A. B. Laursen, P. C. K. Vesborg, O. Hansen, I. Chorkendorff, *J. Am. Chem. Soc.* **2013**, *135*, 1057 – 1064.
[12] C. G. Read, Y. Park, K.-S. Choi, *J. Phys. Chem. Lett.* **2012**, *3*, 1872 – 1876.
[13] S. Ida, K. Yamada, T. Matsunaga, H. Hagiwara, Y. Matsumoto, T. Ishihara, *J. Am. Chem. Soc.* **2010**, *132*, 17343 – 17345.
[14] Y. L. Kim, H. Y. Jung, S. Park, B. Li, F. Liu, J. Hao, Y.-K. Kwon, Y. J. Jung, S. Kar, *Nat. Photonics* **2014**, *8*, 239 – 243.
[15] S. Yasutomi, T. Morita, Y. Imanishi, S. Kimura, *Science* **2004**, *304*, 1944 – 1947.
[16] S. Yasutomi, T. Morita, S. Kimura, *J. Am. Chem. Soc.* **2005**, *127*, 14564 – 14565.
[17] B. Seger, J. McCray, A. Mukherji, X. Zong, Z. Xing, L. Wang, *Angew. Chem. Int. Ed.* **2013**, *52*, 6400 – 6403; *Angew. Chem.* **2013**, *125*, 6528 – 6531.
[18] R. Beranek, H. Kisch, *Angew. Chem. Int. Ed.* **2008**, *47*, 1320 – 1322; *Angew. Chem.* **2008**, *120*, 1340 – 1342.
[19] H. Chen, G. Liu, L. Wang, *Sci. Rep.* **2015**, *5*, 10852.
[20] H. Chen, Q. Wang, M. Lyu, Z. Zhang, L. Wang, *Chem. Commun.* **2015**, *51*, 12072 – 12075.
[21] A. Ortiz, J. C. Alonso, M. García, J. Toriz, *Semicond. Sci. Technol.* **1996**, *11*, 243 – 247.
[22] B. Ghosh, M. Das, P. Banerjee, S. Das, *Appl. Surf. Sci.* **2008**, *254*, 6436 – 6440.
[23] Z. Zainal, M. Z. Hussein, A. Ghazali, *Sol. Energy Mater. Sol. Cells* **1996**, *40*, 347 – 357.
[24] M. Calixto-Rodriguez, H. Martinez, A. Sanchez-Juarez, J. Campos-Alvarez, A. Tiburcio-Silver, M. E. Calixto, *Thin Solid Films* **2009**, *517*, 2497 – 2499.
[25] L. A. Burton, D. Colombara, R. D. Abellon, F. C. Grozema, L. M. Peter, T. J. Savenije, G. Dennler, A. Walsh, *Chem. Mater.* **2013**, *25*, 4908 – 4916.
[26] F. Hanini, A. Bouabellou, Y. Bouachiba, F. Kermiche, A. Taabouche, M. Hemissi, D. Lakhdari, *IOSR J. Eng.* **2013**, *3*, 21 – 28.
[27] G. Wang, Y. Ling, D. A. Wheeler, K. E. N. George, K. Horsley, C. Heske, J. Z. Zhang, Y. Li, *Nano Lett.* **2011**, *11*, 3503 – 3509.
[28] T. Zhou, W. K. Pang, C. Zhang, J. Yang, Z. Chen, H. K. Liu, Z. Guo, *ACS Nano* **2014**, *8*, 8323 – 8333.
[29] P. Boudjouk, D. J. Seidler, G. J. McCarthy, *Chem. Mater.* **1994**, *6*, 2108 – 2112.
[30] W. Albers, C. Haas, H. J. Vink, J. D. Wasscher, *J. Appl. Phys.* **1961**, *32*, 2220 – 2225.
[31] M. Onoda, K. Tada, H. Nakayama, *J. Appl. Phys.* **1999**, *86*, 2110 – 2115.
[32] J. Jasieniak, M. Califano, S. E. Watkins, *ACS Nano* **2011**, *5*, 5888 – 5902.

Manuscript received: November 7, 2016
Revised: December 14, 2016
Accepted Article published: December 16, 2016
Final Article published: ■■ ■■, 0000

© 2017 Wiley-VCH Verlag GmbH & Co. KGaA, Weinheim

*H. Chen, M. Lyu, M. Zhang, K. Feron, D. J. Searles, M. Dargusch, X. Yao, L. Wang**

■■ – ■■

Switched Photocurrent on Tin Sulfide-Based Nanoplate Photoelectrodes

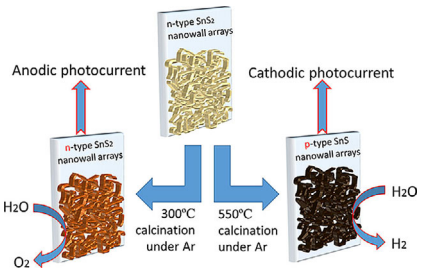

Small plates: A simple chemical method is developed to prepare SnS_2 nanoplate photoelectrodes. Depending on the calcination temperatures, the SnS_2 photoelectrodes can either remain as n-type SnS_2 with greatly enhanced anodic photocurrent or be completely converted into p-type SnS to generate cathodic photocurrent.

© 2017 Wiley-VCH Verlag GmbH & Co. KGaA, Weinheim